Title
Avian egg latebra as brain tissue water diffusion model

Journal
Magnetic Resonance in Medicine, 72(2)

ISSN
0740-3194

Authors
Maier, Stephan E
Mitsouras, Dimitris
Mulkern, Robert V

Publication Date
2014-08-01

DOI
10.1002/mrm.24941

Peer reviewed

Published in final edited form as:
Magn Reson Med. 2014 August ; 72(2): 501–509. doi:10.1002/mrm.24941.

Avian Egg Latebra as Brain Tissue Water Diffusion Model

Stephan E. Maier[†], **Dimitris Mitsouras**[†], and **Robert V. Mulkern**[†,‡]

[†]Department of Radiology, Brigham and Women's Hospital, Harvard Medical School, Boston, MA, 02115

[‡]Department of Radiology, Children's Hospital, Harvard Medical School, Boston, MA, 02115

Abstract

Purpose—Simplified models of non-monoexponential diffusion signal decay are of great interest to study the basic constituents of complex diffusion behaviour in tissues. The latebra, a unique structure uniformly present in the yolk of avian eggs, exhibits a non-monoexponential diffusion signal decay. This model is more complex than simple phantoms based on differences between water and lipid diffusion, but is also devoid of microscopic structures with preferential orientation or perfusion effects.

Methods—Diffusion scans with multiple b-values were performed on a clinical 3 Tesla system in raw and boiled chicken eggs equilibrated to room temperature. Diffusion encoding was applied over the ranges 5–5,000 and 5–50,000 s/mm^2. A low read-out bandwidth and chemical shift was used for reliable lipid/water separation. Signal decays were fitted with exponential functions.

Results—The latebra, when measured over the 5–5,000 s/mm^2 range, exhibited independent of preparation clearly biexponential diffusion, with diffusion parameters similar to those typically observed in in-vivo human brain. For the range 5–50,000 s/mm^2 there was evidence of a small third, very slow diffusing water component.

Conclusion—The latebra of the avian egg contains membrane structures, which may explain a deviation from a simple monoexponential diffusion signal decay, which is remarkably similar to the deviation observed in brain tissue.

Keywords

Diffusion; Biexponential Diffusion; Multiexponential Diffusion; Non-Gaussian Diffusion; Magnetization Transfer; Egg; Latebra; Membrane; Lipid; Coagulation

Introduction

The presence of non-monoexponential water diffusion signal decay in tissues is well established [1–8]. A fully satisfying explanation for this deviation or a correct attribution of compartments in the case of the physically motivated biexponential model [2] has to date not been achieved [9]. A major obstacle in the interpretation of data is the complexity of

Address for Correspondence: Stephan E. Maier, MD, PhD, Radiology (MRI), Brigham and Women's Hospital, Harvard Medical School, 75 Francis Street, Boston, MA 02115, Tel: 617 - 732-5065, Fax: 617 - 264-5275, stephan@bwh.harvard.edu.

tissue, not only at the level of imaging voxels but also at the level of individual cells. It is quite clear that the presence of cell and organelle membranes and the consequential hindrance and compartmentalization of the diffusion process is fundamentally linked with the observed deviation from the monoexponential diffusion signal decay observed in simple fluids. It is thus of great interest to study simplified models, which also exhibit non-monoexponential diffusion. One of the most simple models for studying the complex aspects of tissue diffusion is a mixture of fat and water, such as dairy cream [10,11]. This model produces true biexponential diffusion signal decays. However, the underlying mechanism of vastly different diffusion within suspended lipid droplets and surrounding water evidently has nothing in common with the physical cause for non-monoexponential diffusion signal decay observed in tissues. Other model systems, which contains more tissue-like intra- and extracellular compartments that rapidly exchange water molecules, are blood [12] and isolated blood cells [13].

Here we present avian eggs as an easily accessible water diffusion model that also has more in common with tissue water diffusion than the aforementioned dairy cream model. The general MR imaging and relaxation properties of hen eggs have previously been studied by Jayasundar et al [14] and Laghi et al [15]. In particular, Jayasundar et al demonstrated that all the internal structures of an unfertilized egg [16], including the protein-rich egg white with chalaza and the lipid-rich layered egg yolk can readily be visualized by MR imaging. Also visible on MR images is a central flask shaped structure called the latebra [17], which is visually distinguished from the rest of the yolk by its white colour and more fluid nature [18]. A narrow column of white yolk connects the latebra to the nucleus of Pander, which is beneath the blastodisc, where ultimately the embryo develops.

We report water diffusion measurements of the latebra and show with multi-component analysis how water diffusion in the latebra is distinctly different from water diffusion within the egg white. We also examine how the act of cooking eggs affects the diffusion properties.

Methods

Chicken eggs, known to be unfertilized, were purchased at local groceries. Some of the eggs were boiled in water for 5 or 15 minute periods, respectively. Boiled and refrigerated raw eggs were allowed to equilibrate inside the scanner room to ambient temperatures for at least 24 hours before scanning. Imaging was performed on a GE Medical Systems clinical 3 Tesla Signa HDxt scanner. For each configuration, i.e., raw, 5 and 15 minute boiled, a total of eight eggs were studied. Diffusion data of vials containing water and olive oil were obtained for reference. For the experimental setup, four eggs were placed inside a 10 centimeter diameter bird-cage wrist coil in a quadrilateral arrangement. Axial image planes resulted in images showing two eggs simultaneously. Optimal axial slice positions through the centrally located latebra of each egg were determined with the help of localizing scans. Line scan diffusion imaging (LSDI) [19, 20] was used to acquire diffusion-weighted images with a 200 mm field of view, a TR of 3,000 ms and three orthogonal diffusion encoding directions at 16 evenly spaced *b*-values. A first diffusion data set was obtained with diffusion weightings between 5 and 5,000 s/mm^2 (3 mm slice thickness, 128×128×0.5 matrix, 85 ms TE, δ=23.9 ms, Δ=41.9 ms). The diffusion data was acquired both with and without a

magnetization transfer (MT) pulse at a 1,200 Hz frequency offset, to investigate if bound water is in preferred exchange with slow diffusion water pools. A second diffusion data set was collected with diffusion weightings over a ten times larger range, i.e., between 5 and 50,000 s/mm^2 (6 mm slice thickness, 64×64×0.5 matrix, 144 ms TE, δ=61.4 ms, Δ=71.9 ms). For each scan, the shortest possible echo time was selected. Simultaneous switching of the main axis magnetic field gradients at respective relative amplitudes of 1.0, 1.0, and 0.5 of the maximum allowable amplitude resulted in a maximum amplitude of 60 mT/m. A very low read-out bandwidth of ±2.4 kHz produced SNR with sufficient signal even for the highest *b*-values measured as well as very reliable water/lipid separation based on the dislocation that resulted from the water/lipid chemical shift. Image data were processed off-line with dedicated software. The geometric mean $\overline{S}=\sqrt[3]{S_1S_2S_3}$ of the diffusion signals measured along the three orthogonal diffusion encoding directions was used to fit the diffusion signal decay. Only signal values that exceeded a threshold equal to three times the average magnitude background signal were used. Exponential fitting was accomplished with a nonlinear least-squares Levenberg-Marquardt algorithm. For the high-*b* ($5 \le b \le 5{,}000$ s/mm^2) diffusion data, fitting was performed for each individual pixel followed by region-of-interest (ROI) analysis of the resulting maps. Biexponential tissue diffusion parameters were obtained by fitting the mean signal intensity decay $\overline{S}$ vs *b*-value to a biexponential function of the form

$$\overline{S}(b)=A_1\exp(-D_1b)+A_2\exp(-D_2b), \quad (1)$$

where D_1 and D_2 describe the diffusion coefficients of fast and slow diffusion components, respectively, and A_1 and A_2 the signal contribution of each component. The ratios $A_1/(A_1+A_2)$ and $A_2/(A_1+A_2)$ define the size fractions f_1 and f_2 of the fast and slow diffusion component, respectively. For the very high-*b* ($5 \le b \le 50{,}000$ s/mm^2) diffusion data, fitting was performed with average signal values measured within the ROI. Average signals measured within the latebra were fitted with a triexponential function with three diffusion coefficients D_1, D_2, and D_3 and their respective size fractions f_1, f_2, and f_3. In addition, the slowest diffusion component D_3^M was estimated by applying a monoexponential fit exclusively to the average diffusion signals measured at *b*=20,003 s/mm^2 and above. The respective relative signal fraction f_3^M was estimated by extrapolating the monoexponential fit to *b*=5 s/mm^2 and scaling it with the measured signal at *b*=5 s/mm^2. Yolk lipid diffusion was estimated by monoexponential fitting. To avoid signal contamination from eggwhite water components, only diffusion signals measured at *b*=6,671 s/mm^2 and above were considered.

Ambient temperature was measured during each scan session. Measurements that showed monoexponential water diffusion were temperature corrected assuming a reference temperature of 20 C [21]. Statistical differences were assessed with a two-sided *t*-test with levels of $p \le 0.05$ considered significant.

Results

An example of a localizer image showing the basic egg structures, i.e., egg white, yolk and latebra, is presented in Fig. 1a. The average diameter of the latebra determined on the localizing scans of raw eggs was 3.1±0.9 mm. Diffusion-weighted images obtained with LSDI are shown in Figs, 1b through f. Images b, c and d were obtained with the high-*b* diffusion scan, whereas images e and f were acquired with the very high-*b* diffusion scan, which compared to the high-*b* diffusion scan was performed at lower resolution and at a longer echo time. Typical examples of maps produced by biexponential pixel-by-pixel analysis of high-*b* diffusion data are presented in Fig. 2.

Representative signal decays observed with the high-*b* and very high-*b* diffusion scans in the latebra of raw and boiled eggs are displayed in Fig. 3. The diffusion signal measured in the latebra ROI over the *b*-value range 5–5,000 s/mm^2 exhibits a pronounced deviation from a simple monoexponential decay (see Fig. 3A). A separate, very slow diffusing component is revealed at *b*-values above 20,000 s/mm^2 (see Fig. 3B).

Average diffusion biexponential signal fit parameters for the latebra with and without the application of an MT pulse and MT-ratios $(S_{off}–S_{on})/S_{off}$ are given in Table 1. Results of triexponential and monoexponential slow-component analysis of the very high diffusion-weighted latebra data are shown in Table 2. For raw eggs and eggs that had been boiled for 5 minutes, triexponential fits converged consistently. Judged by the residuals and likewise by simple visual inspection of the fitted curve and it's relation to the original data, triexponential fits were always superior to biexponential fits. For the eggs that had been boiled for 15 minutes, triexponential fitting convergence could not always be attained and values are therefore not reported. All diffusion coefficients consistently presented the highest value after short boiling and the lowest value after extended boiling. However, differences were not always statistically significant. The fast diffusion signal fraction f_1 decreased with boiling time and conversely the slow and very slow diffusion signal fractions f_2 and f_3 increased with boiling time. As for the diffusion coefficients, these observed differences were also not always statistically significant. Pairwise comparisons of measurements made with and without MT pulse revealed significant differences in raw eggs only. It was remarkable, however, how independent of egg preparation, the application of an MT pulse consistently caused an increase of D_1, D_2 and f_2 and a decrease of f_1. The effect of the MT pulse on the very slow diffusion coefficient appeared to be subtle and, given the large statistical variation, difficult to detect. A comprehensive investigation was therefore not performed.

Characteristic diffusion signal decay curves measured in the egg white of raw and boiled eggs are displayed in Fig. 4. Fitting of the diffusion data appeared to indicate monoexponential diffusion signal decays irrespective of preparation. However, closer inspection of the signal decay curves for boiled egg white in Fig. 4 shows that the last four signals measured above the noise threshold also lie above the fitted line. This seems to indicate the presence of a small slow diffusion component. Average MT ratios and water ADC values obtained with monoexponential fitting of the egg white signal decays in eight eggs are listed in Table 3. The highest ADC occurred in raw egg white. Boiling caused a

small but significant reduction of the ADC and a four-fold increase of the MT-ratio. However, boiling duration appeared to have no significant effect on both ADC and MT ratio. There was also no significant difference between ADC values measured without and with MT pulse.

Examples of the lipid signal decay observed in the yolk of a raw egg and an egg that underwent 5 minutes of boiling are shown in Fig. 5. In raw eggs, yolk lipid diffusion equaled 0.67±0.22 $nm^2/\mu s$ and in eggs exposed to 5 minutes of boiling, 0.70±0.33 $nm^2/\mu s$. Remarkable was a more than twofold increase of the lipid signal in the boiled eggs compared to the lipid signal of the raw eggs (see Fig. 5). In eggs that had been boiled for 15 minutes, there was no clear tendency for signal loss with increasing diffusion weighting and, therefore, diffusion coefficients could not be determined.

Ambient temperatures for the high-*b* scans varied between 18 and 21.5 C with an average of 19.4±1.8 C. Since scans with and without MT pulse were performed sequentially, there was no significant temperature change contributing to the MT experiments. For the very high-*b* diffusion scans, ambient temperatures varied between 17 and 18 C with an average of 17.4±0.4 C.

Decay curves of the diffusion imaging experiments performed with samples of tap water and olive oil are presented in Fig. 6. The water diffusion coefficient was 1.975 $\mu m^2/ms$ at 17.5 C. After numerical adjustment to a temperature of 20 C [21], the water diffusion coefficient equaled 2.118 $\mu m^2/ms$. The diffusion coefficient for olive oil measured at 17.5 C was 7.95 $nm^2/\mu s$. The MR signal of the olefinic groups residing on the lipid molecules was found to be well above baseline noise for the entire range of *b*-values up to 50,000 s/mm^2. Analysis of the olefinic group diffusion signal decay yielded a diffusion coefficient of 6.66 $nm^2/\mu s$.

Discussion

Latebra: Non-Monoexponential Diffusion Properties

It is remarkable that signal values measured in the latebra (see Fig. 3), unlike signal values measured in egg white (see Fig. 4) or water (see Fig. 6), appear well above the noise threshold for all investigated *b*-values. The limited spatial resolution in relation to the size of the latebra might give rise to partial volume effects. However, this concern is largely mitigated by the observation that latebra water signals exceeded yolk water signals by many times. Thus the obvious deflection from a pure monoexponential signal decay is not related to low signal, but rather to intrinsic diffusion properties of the latebra. To the best of our knowledge this is the first study demonstrating that within the latebra of the avian egg, the diffusion signal decay is better characterized by a non-monoexponential than a monoexponential function. Biexponential analysis results in a fast diffusion coefficient that is 37% lower than the ADC of tap water. The boiling time dependence of the diffusion parameters may indicate the degree of denaturation and coagulation in the central portion of the egg. The biexponential diffusion coefficients and signal fractions of the latebra are remarkably similar to those observed in brain [2,22]. However, a major difference between the present latebra data and in-vivo human data is the temperature. It can be expected that latebra diffusion coefficients at normal body temperature instead of room temperature would

be significantly higher. Albeit, it is not clear if signal fractions would be different and diffusion coefficients would increase by the same proportion. A complicating factor of tissue diffusion signal decay at lower *b*-values, which is of course absent in the case of unfertilized eggs, is the effect of perfusion. Application of an MT pulse introduced only a small signal loss, which did not change after boiling. The effect of the MT pulse on the diffusion parameters appears to be consistent, but very small. Exactly the same pattern of biexponential diffusion parameter changes, i.e., increase of D_1, D_2 and f_2 and decrease of f_1 was observed by Ronen et al in cat brain [23]. Experiments performed in human brain on a clinical scanner by Mulkern et al [24] revealed no significant changes and appear to agree with the present finding that the effect is very small, at least under the experimental limitations encountered with MT pulses on clinical scanners.

Latebra: Very Slow Diffusion Beyond a Biexponential Signal Decay

The presence of a third, very slow diffusion component, with a diffusion coefficient that is more than a magnitude lower than the diffusion coefficient of the slow diffusion component and about two magnitudes lower than the diffusion coefficient of the fast diffusion component, is remarkable. Of course, due to differences in echo time and diffusion encoding time the two diffusion measurements can not be directly related to each other. However, the more rapid non-monoexponential decay at *b*-values below 10,000 s/mm^2 is also visible in the data obtained at very high diffusion weighting. With the present values of the biexponential water diffusion coefficients D_1 and D_2, hypothetical signal contributions from these components at or above b=20,000 s/mm^2 would be more than an order of magnitude smaller than the actually observed signal. Thus, slow diffusion can be measured with a separate monoexponential fit of only the higher *b*-values. Moreover, the diffusion coefficient measured for triglycerides in vegetable oil is consistent with literature values [25–27] and confirms that very high diffusion weighting can be performed on the clinical system used in this study. Nonetheless, the finding of a diffusion coefficient in the latebra that is similar to the diffusion coefficient of triglycerides in vegetable oil does raise the question if the observed signal is simply due to contamination by chemical shift artifacts. The egg white indeed contains some lipids that might interfere with the present measurement. However, these lipids constitute only 0.03% [28], i.e., a minute amount of the water-dominated egg white mass, which is too little to explain the observed signal fraction of several percent. A contamination by signal from triglycerides in the yolk can firmly be excluded based on spatial separation. However, the olefinic protons, which constitute between 5 to 10% of all lipid protons, are characterized by a 5.4 ppm chemical shift signal that is close to that of water protons (4.7 ppm) [29]. Thus, for the low resolution diffusion data contamination of latebra water signal by the olefin signal is likely, since the spatial olefin signal shift with respect to water equals 2.4 pixels, i.e., a distance of 7.5 mm. We believe, however, that the third and slowest component in the triexpoential fit of the latebra diffusion data rises largely from a water component, since it's diffusion coefficient is an order of magnitude larger than diffusion coeffcients of the MR-observable triglyceride protons in the yolk. The olive oil experiments confirmed that diffusion of the olefin groups can be measured and that their diffusion coefficient is in reasonable agreement with the diffusion coefficient of the methyl/methylene protons of the lipids. For the olive oil experiments, contribution of the water MR signal was not of concern, due to a relative weight water content of typically well below 1%

[30]. The lipid diffusion in yolk was a magnitude smaller than lipid diffusion in olive oil and than the slowest diffusion observed in the latebra. Despite diffusion weighting of up to 50,000 s/mm^2, a signal loss of only a few percent could be invoked, which resulted in somewhat unreliable determination of the diffusion coefficient. The higher lipid signal in eggs that had been boiled is in agreement with the observation by Fieremans et al that after heat treatment fat protons in cream exhibit a longer transverse relaxation time [11]. To estimate the contamination by olefins, biexponential fits over the range 20,000–50,000 s/mm^2 were also performed, assuming a mixture of water/olefin with the lipid diffusion coefficient as an independently measured diffusion parameter. Obviously, the increased number of parameters and the relatively minor signal decay resulted in much less stable fitting. For raw eggs, this fitting produced a olefin signal fraction of 0.031±0.019, a manyfold increased water diffusion coefficient of 0.079±0.034 μm^2/ms and an increased water signal fraction f_3 of 0.087±0.058. Similarly, for eggs that had been boiled for 5 minutes, the olefin signal fraction amounted to 0.021±0.013, the water diffusion coefficient increased to 0.066±0.032 μm^2/ms and the water signal fraction f_3 increased to 0.094±0.069. Overall, it seems the water diffusion in the latebra is better characterized with more than two diffusion coefficients. This observation also supports the notion of a asymmetrically distributed spectrum of diffusion coefficients [31] rather than distinct water components.

Egg White

The diffusion measurements in the water rich egg white confirm earlier results of monoexponential water diffusion [32,33]. Though in cooked egg white, decay curves seemed to hint at the presence of a slow diffusion signal component, which appeared to just barely rise above the Rician noise distribution. Thus the question arises, which are the unique differences between egg white and latebra that cause such remarkable differences in diffusion?

Diffusion in View of Egg Composition and Egg Micro Structure

Egg white consists primarily of water. The bulk of the remaining 12% weight are albumen proteins [28]. The main albumen constituents are proteins, such as ovalbumin (54%), with relatively low molecular weights between 28,000 and 76,000 Da [28]. In raw egg white, compared to tap water, the reduction of the water diffusion coefficient by 17% indicates that the proteins pose a relatively small obstacle to the diffusion process. During boiling, heat-induced coagulation occurs, i.e., a change from a fluid (sol) to a solid or semisolid (gel) state. Coagulation involves changes in the structure of the egg protein molecules. During the initial denaturation, disulfide bonds are formed and hydrophobic groups are exposed. After further heating, the denatured protein molecules aggregate randomly. The aggregation causes a dramatic change in the mechanical properties of egg white [28], but the consequential reduction of water diffusion amounts only to another 5%. This small change in diffusion also stands in stark contrast with the observed four-fold increase of the MT-ratio.

In contrast, egg yolk, of which the latebra constitutes a component, is a profoundly complex substance with approximately 50% water content, 34% lipids, 16% proteins and minor amounts of carbohydrates and minerals [28]. Lipids are present in the form of lipoprotein

droplets that range in size from 2 to 10 μm [16]. White yolk, which is found inside the latebra but also as narrow bands within the layered yellow yolk, is characterized by a lower lipid and higher water content [34]. Unfortunately, according to Bellairs [16], no satisfactory technique has been devised for separating the yellow and white yolk completely, thus chemical analyses are bound to be problematic. The MR image data in Fig. 1 shows very low water signal in the areas with predominantly yellow yolk and relatively high water signal within the white yolk-containing latebra. On the other hand, low signal in the center of the shifted yellow yolk signal seen in Fig. 1a is in agreement with a lower lipid content of the latebra. Another gross component of white and yellow yolk are yolk spheres [35]. These spheres contain lipid sub-droplets and aqueous protein fluid. The white yolk spheres vary in diameter from about 4 μm to 75 μm and the yellow yolk spheres from about 25 μm to 150 μm [36]. Bellairs [35], using electron microscopic imaging, concluded that the spheres are surrounded by membranes, but cautioned that these membranes can not be considered completely comparable to cell membranes. It has also been suggested that these membranes resemble myelin figures, which can form spontaneously by hydration of phospholipids present in egg yolk [18, 35]. Mineki and Kobayashi [37] demonstrated with electron microscopy of freeze-cut fixated specimens that the spheres are closely packed and rather polygonal in shape. Woodward and Cotterill [38] also observed polyhedra in cooked egg yolk and attribute the crumbly texture of cooked egg yolk to the internal microstructure. In a review about the organization of egg yolk components Shenstone [39] pointed out that the rate of water diffusion between egg white and yolk was much lower than expected from the respective osmolarities and probably hindered by some structural arrangement within the yolk. Taken together, all these facts seem to provide intriguing reasons for an environment with hindered and restricted diffusion, which would explain the observed non-monoexponential water diffusion. The size of the spheres or polyhedra in white yolk falls in the range of cell sizes encountered in tissues. Given the rather long diffusion encoding times resulting from the clinical system used in the present study, it is possible that water molecules exhibit diffusion anomalies caused by entrapment within or between the spherical or polygonal structures. Indeed, theoretical analysis of data collected under the requisite condition $\delta \ll \Delta$, as discussed by Callaghan et al [40], may ultimately elucidate microstructural details of the latebra and yolk. Larger spheres, as they are encountered in the yellow yolk, should present less hindrance. Unfortunately, water diffusion in the yellow yolk could not be quantified in this study due to exceedingly low signal, probably as a result of the lower water content and short transverse relaxation times. Obviously, lipid droplets also present obstacles that hinder diffusion. However, given the lower lipid content of white yolk, lipid droplets may not be dense enough to cause a substantial entrapment of water molecules over time periods that correspond to the diffusion time $\Delta - \delta/3$. This mechanism might be of greater importance in yellow yolk, where lipid concentration is higher. As already stated above, data to confirm or challenge such speculation was not available due to the low water signal in the yolk under the present experimental conditions. Finally, it has been suggested that water molecules trapped among macro-molecules, which are embedded in cell and organelle membranes, may constitute the observed slow diffusion component in tissues [41]. The present egg model, which certainly does not contain such complex membrane structures, proves that this mechanism is not conditional for a biexponential diffusion signal decay.

Conclusion

The avian egg presents a simple but relevant object for exploring biophysical aspects of water diffusion. Other relevant objects for this purpose have been suggested, including dairy cream phantoms [10, 11], blood [12] and erythrocyte ghost preparations [13]. However, the water diffusion signal decay within the latebra is strikingly similar to what is observed in human brain tissue when examined over a wide range of *b*-values and can, therefore, be used as a reference in the investigation of new diffusion imaging pulse sequences. Limitations of this model are the small size, which makes difficult to attain sufficient SNR and avoid partial volume effects, particularly at shorter echo times. The cross-linking of proteins with cooking has no major effect on water diffusion in the latebra or egg white. The observation of a third diffusion component in the latebra is remarkable and we believe is best explained by the existence of water in a highly restricted environment. The presence of olefins, which share chemical shift close to water could also produce a slow diffusion component, but would be expected to diffuse at the much slower rate for triglyceride protons in general. Our findings in the latebra, which is available for correlative histological and/or submicroscopic methods, may help ellucidate poorly understood factors leading to non-monoexponential diffusion decays in tissues.

Acknowledgments

The research presented in this paper was supported by research grants from the National Institute of Biomedical Imaging (R01 EB006867 and R01 EB10195 to S.E.M.) and National Cancer Institute (R01 CA160902 to S.E.M.), a resource grant funded jointly by the National Center for Research Resources, the National Cancer Institute, and the National Institute of Biomedical Imaging (U41 RR019703), and a K-award from the National Institute of Biomedical Imaging (K01 EB015868 to D.M.).

References

1. Niendorf T, Dijkhuizen RM, Norris DG, van Lookeren Campagne M, Nicolay K. Biexponential diffusion attenuation in various states of brain tissue: Implications for diffusion-weighted imaging. Magn Reson Med. 1996; 36(6):847–857. [PubMed: 8946350]
2. Mulkern RV, Gudbjartsson H, Westin CF, Zengingonul HP, Gartner W, Guttmann CR, Robertson R, Kyriakos W, Schwartz R, Holtzman D, Jolesz FA, Maier SE. Multi-component apparent diffusion coefficients in human brain. NMR in Biomedicine. 1999; 12:51–62. [PubMed: 10195330]
3. Mulkern RV, Vajapeyam S, Robertson RL, Caruso PA, Rivkin MJ, Maier SE. Biexponential apparent diffusion coefficient parametrization in adult vs newborn brain. Magn Reson Imaging. 2001; 19(5):659–668. [PubMed: 11672624]
4. Clark CA, Hedehus M, Moseley ME. In vivo mapping of the fast and slow diffusion tensors in human brain. Magn Reson Med. 2002; 47(4):623–8. [PubMed: 11948721]
5. Bennett KM, Schmainda K, Bennett R, Rowe D, Lu H, Hyde J. Characterization of continuously distributed cortical water diffusion rates with a stretched-exponential model. Magn Reson Med. 2003; 50(4):727–34. [PubMed: 14523958]
6. Maier SE, Vajapeyam S, Mamata H, Westin CF, Jolesz FA, Mulkern RV. Biexponential diffusion tensor analysis of human brain diffusion data. Magn Reson Med. 2004; 51(2):321–330. [PubMed: 14755658]
7. Jensen JH, Helpern JA, Ramani A, Lu H, Kaczynski K. Diffusional kurtosis imaging: the quantification of non-gaussian water diffusion by means of magnetic resonance imaging. Magn Reson Med. 2005; 53(6):1432–40. [PubMed: 15906300]

8. Mulkern RV, Barnes AS, Haker SJ, Hung YP, Rybicki FJ, Maier SE, Tempany CM. Biexponential characterization of prostate tissue water diffusion decay curves over an extended b-factor range. Magn Reson Imaging. 2006; 24(5):563–8. [PubMed: 16735177]
9. Mulkern RV, Haker SJ, Maier SE. On high b diffusion imaging in the human brain: Ruminations and experimental insights. Magn Reson Imaging. 2009; 27(8):1151–62. [PubMed: 19520535]
10. Ababneh Z, Haque M, Maier SE, Mulkern RV. Dairy cream as a phantom material for biexponential diffusion decay. MAGMA. 2004; 17(2):95–100. [PubMed: 15526227]
11. Fieremans E, Pires A, Jensen JH. A simple isotropic phantom for diffusional kurtosis imaging. Magn Reson Med. 2012; 68(2):537–42. [PubMed: 22161496]
12. Li JG, Stanisz GJ, Henkelman RM. Integrated analysis of diffusion and relaxation of water in blood. Magn Reson Med. 1998; 40(1):79–88. [PubMed: 9660557]
13. Thelwall PE, Grant SC, Stanisz GJ, Blackband SJ. Human erythrocyte ghosts: Exploring the origins of multiexponential water diffusion in a model biological tissue with magnetic resonance. Magn Reson Med. 2002; 48(4):649–57. [PubMed: 12353282]
14. Jayasundar R, Ayyar S, Raghunathan R. Proton resonance imaging and relaxation in raw and cooked hen eggs. Magn Reson Imaging. 1997; 15(6):709–717. [PubMed: 9285811]
15. Laghi L, Cremonini MA, Placucci G, Sykora S, Wright K, Hills B. A proton NMR relaxation study of hen egg quality. Magn Reson Imaging. 2005; 23(3):501–510. [PubMed: 15862652]
16. Bellairs R. Biological aspects of the yolk of the hen's egg. Adv Morphog. 1964; 4:217–272. [PubMed: 5331923]
17. Falen SW, Szeverenyi NM, Packard DSJ, Ruocco M. Magnetic resonance imaging study of the structure of the yolk in the developing avian egg. J Morphol. 1991; 209(3):331–42. [PubMed: 1942074]
18. Bain JM, Hall JM. Observations on the development and structure of the vitelline membrane of the hen's egg: an electron microscope study. Aust J Biol Sci. 1970; 23(3):657–72.
19. Gudbjartsson H, Maier SE, Mulkern RV, Mórocz IÁ, Patz S, Jolesz FA. Line scan diffusion imaging. Magn Reson Med. 1996; 36(4):509–519. [PubMed: 8892201]
20. Maier SE, Gudbjartsson H, Patz S, Hsu L, Lovblad KO, Edelman RR, Warach S, Jolesz FA. Line scan diffusion imaging: Characterization in healthy subjects and stroke patients. Am J Roentgen. 1998; 17(l):85–93.
21. Le Bihan D, Delannoy J, Levin RL. Temperature mapping with MR imaging of molecular diffusion: Application to hyperthermia. Radiology. 1989; 171(3):853–7. [PubMed: 2717764]
22. Maier SE, Mulkern RV. Biexponential analysis of diffusion related signal decay in normal human cortical and deep gray matter. Magn Reson Imaging. 2008; 26(7):897–904. [PubMed: 18467062]
23. Ronen I, Moeller S, Ugurbil K, Kim DS. Investigation of multicomponent diffusion in cat brain using a combined MTC-DWI approach. Magn Reson Imaging. 2006; 24:425–431. [PubMed: 16677949]
24. Mulkern RV, Vajapeyam S, Haker SJ, Maier SE. Magnetization transfer studies of the fast and slow tissue water diffusion components in the human brain. NMR in Biomedicine. 2005; 18(3): 186–94. [PubMed: 15578729]
25. Guillermo A, Bardet M. In situ pulsed-field gradient NMR determination of the size of oil bodies in vegetable seeds, analysis of the effect of the gradient pulse length. Anal Chem. 2007; 79:6718–26. [PubMed: 17655200]
26. Ababneh ZQ, Beloeil H, Berde CB, Ababneh AM, Maier SE, Mulkern RV. In vivo lipid diffusion coefficient measurements in rat bone marrow. Magn Reson Imaging. 2009; 27(6):859–64. [PubMed: 19167181]
27. Steidle G, Eibofner F, Schick F. Quantitative diffusion imaging of adipose tissue in the human lower leg at 1.5 T. Magn Reson Med. 2011; 65(4):1118–24. [PubMed: 21413077]
28. Stadelman, WJ.; Cotterill, OJ. Egg Science and Technology. 4. The Haworth Press, Inc; Binghamton, NY: 1995.
29. Hernando D, Karampinos DC, King KF, Haldar JP, Majumdar S, Georgiadis JG, PLZ. Removal of olefinic fat chemical shift artifact in diffusion mri. Magn Reson Med. 2011; 65(3):692–701. [PubMed: 21337402]

30. Hatzakis E, Dais P. Determination of water content in olive oil by 31P NMR spectroscopy. J Agric Food Chem. 2008; 56(6):1866–72. [PubMed: 18303819]

31. Yablonskiy DA, Bretthorst GL, Ackerman JJ. Statistical model for diffusion attenuated MR signal. Magn Reson Med. 2003; 50(4):664–9. [PubMed: 14523949]

32. James TL, Gillen KT. Nuclear magnetic resonance relaxation time and self-diffusion constant of water in hen egg white and yolk. Biochim Piophys Acta. 1972; 286(1):10–15.

33. Graham SJ, Stanisz GJ, Kecojevic A, Bronskill MJ, Henkelman RM. Analysis of changes in MR properties of tissues after heat treatment. Magn Reson Med. 1999; 42(6):1061–1071. [PubMed: 10571927]

34. Riddle O. On the formation, significance and chemistry of the white and yellow yolk of ova. J Morphol. 1911; 22(2):455–491.

35. Bellairs R. The structure of the yolk of the hen's egg as studied by electron microscopy. I. the yolk of the unincubated egg. J Biophys Biochem Cytol. 1961; 11:207–225. [PubMed: 13866859]

36. Romanoff, AL.; Romanoff, AJ. The Avian Egg. J. Wiley and Sons; New York, NY: 1949.

37. Mineki M, Kobayashi M. Microstructure of yolk from fresh eggs by improved method. J of Food Sci. 1997; 62(4):757–761.

38. Woodward SA, Cotterill OJ. Texture and microstructure of cooked whole egg yolks and heat formed gels of stirred egg yolk. J of Food Sci. 1987; 52(1):63–67.

39. Shenstone, FS. The gross composition, chemistry and physiochemistrical basis of organization of the yolk and white. In: Carter, TC., editor. Egg Quality A Study of the Hen's Egg. Oliver and Boyd; Edingburgh: 1968. p. 26-58.

40. Callaghan PT, Godefroy S, Ryland BN. Diffusion-relaxation correlation in simple pore structures. J Magn Reson. 2003; 162(2):320–7. [PubMed: 12810015]

41. Le Bihan D. The "wet mind": Water and functional neuroimaging. Phys Med Biol. 2007; 52(7):R57–90. [PubMed: 17374909]

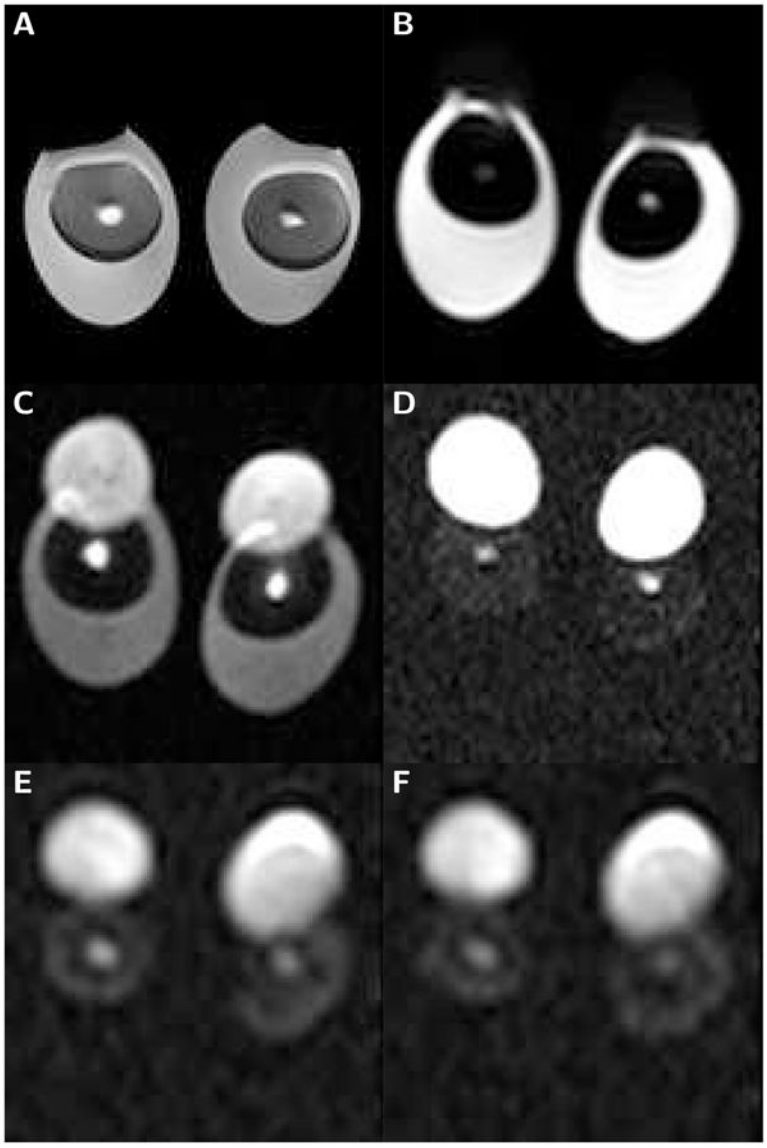

Figure 1.

Sub-images (100 mm field of view) of boiled and raw egg-pairs scanned with the localizing sequence and LSDI. The brightness of the individual images has been adjusted for optimal viewing. A) Spin-echo image (TE=30 ms) of eggs boiled for 5 minutes. B) High-resolution line scan diffusion image (b=5 s/mm^2) of raw eggs. C) High-resolution line scan diffusion image (b=2,000 s/mm^2) of raw eggs. D) High-resolution line scan diffusion image (b=5,000 s/mm^2) of raw eggs. E) Low-resolution line scan diffusion image (b=20,000 s/mm^2) of raw eggs. F) Low-resolution line scan diffusion image (b=50,000 s/mm^2) of raw eggs. The latebra is clearly visible as a bright structure in the center of the yolk. It evidently maintains signal above noise, even at a b-value of 50,000 s/mm^2. In contrast, already at 5,000 s/mm^2 the water signal of the egg white falls well below the noise threshold. On the diffusion-weighted images the lipid containing portion of the yolk is shifted upwards, permitting an unencumbered water diffusion analysis of the latebra.

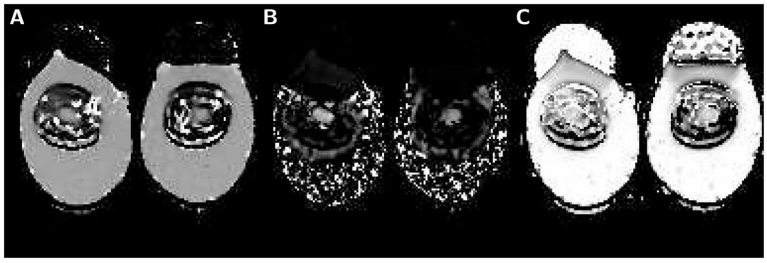

Figure 2.

Maps obtained with biexponential analysis of high-*b* diffusion data measured in eggs that underwent 15 minutes of boiling. A) Map of the fast diffusion coefficient D_f. In egg white, D_f equals 1.68 μm^2/ms (left egg) and 1.70 μm^2/ms (right egg). In the latebra, D_f equals 1.50 μm^2/ms (left egg) and 1.45 μm^2/ms (right egg). B) Map of the slow diffusion coefficient D_s. In egg white, slow diffusion coefficient values can not be determined since the slow diffusion component is very small or not present. In contrast, in the latebra there is clear evidence of biexponential diffusion signal decay with a substantial slow diffusion component. D_s equals 0.30 μm^2/ms (left egg) and 0.23 μm^2/ms (right egg). C) Map of the fast diffusion component size fraction f_1 In most of the egg white, f_1 is very close to one (0.99 for left egg and 0.97 right egg), indicative of purely monoexponential diffusion signal decay. Within the upper portion of the egg white there is an area, where the overlapping signal of yolk lipid produces a biexponential diffusion signal decay with f_1 clearly lower than one. In the latebra, f_1 is also distinctly smaller than one (0.75 for the left egg and 0.78 for the right egg), indicative of a non-monoexponential diffusion signal decay. Finally, there is evidence of ringing artifacts along the edge of the egg white.

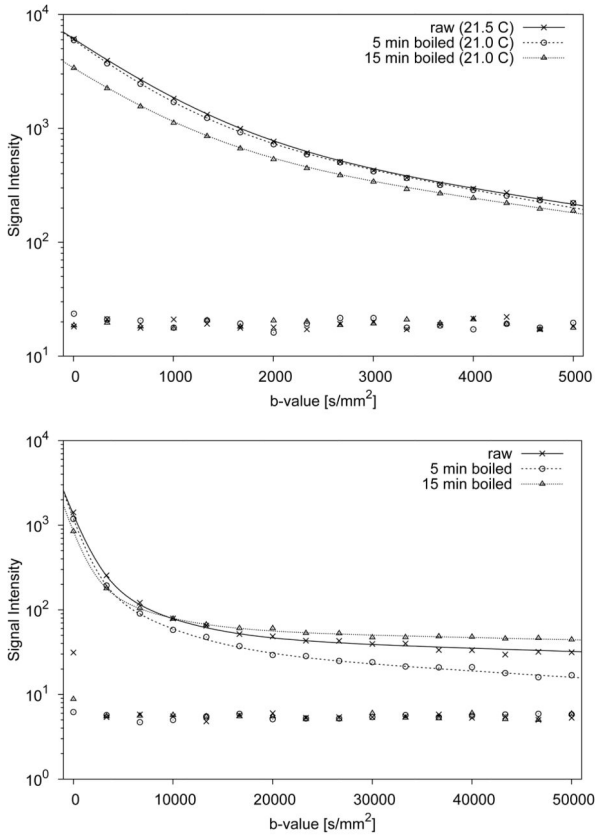

Figure 3.

Typical examples of diffusion signal decays measured in latebra ROIs of raw and boiled chicken eggs. The data shown in the top graph were obtained with high diffusion weighting ($5 \leq b \leq 5{,}000$ s/mm^2), whereas the data shown in the bottom graph were obtained with very high diffusion weighting ($5 \leq b \leq 50{,}000$ s/mm^2). For each *b*-value, average background noise values are also shown. Continuous lines represent fits through the signal decay data. In the range $5 \leq b \leq 5{,}000$ s/mm^2, biexponential fits appear to well describe the signal decay. For the higher diffusion range, triexponential functions produce superior fits.

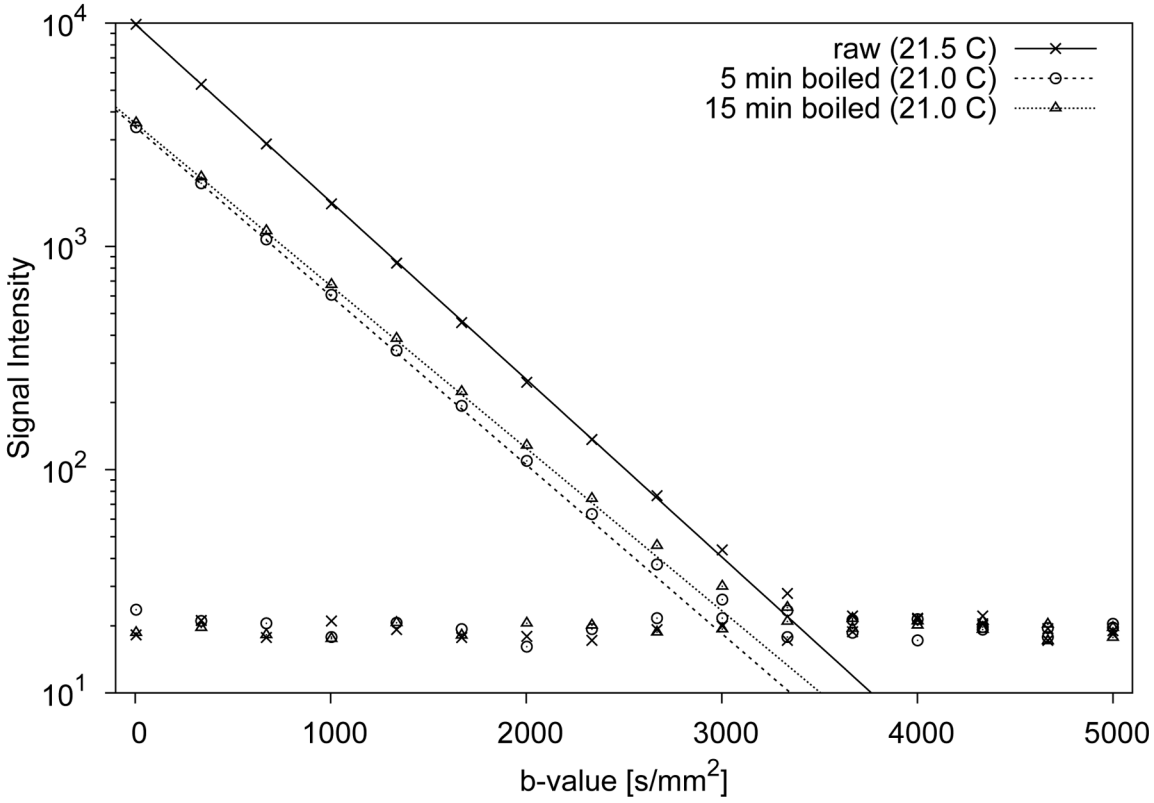

Figure 4.

Representative diffusion signal decays measured in egg white ROIs of raw and boiled eggs. Continuous lines represent monoexponential fits through the signal decay data. For each *b*-value, average background noise values are also provided. For *b*-values above 3,500 s/mm^2, the signal in egg white falls below the noise threshold. Boiling causes only a small decrease in water diffusion, which, given the narrow range of temperatures under which the experiments were performed, can not be explained by changes in temperature. Extension of the boiling time from 5 to 15 minutes appears to have no significant effect.

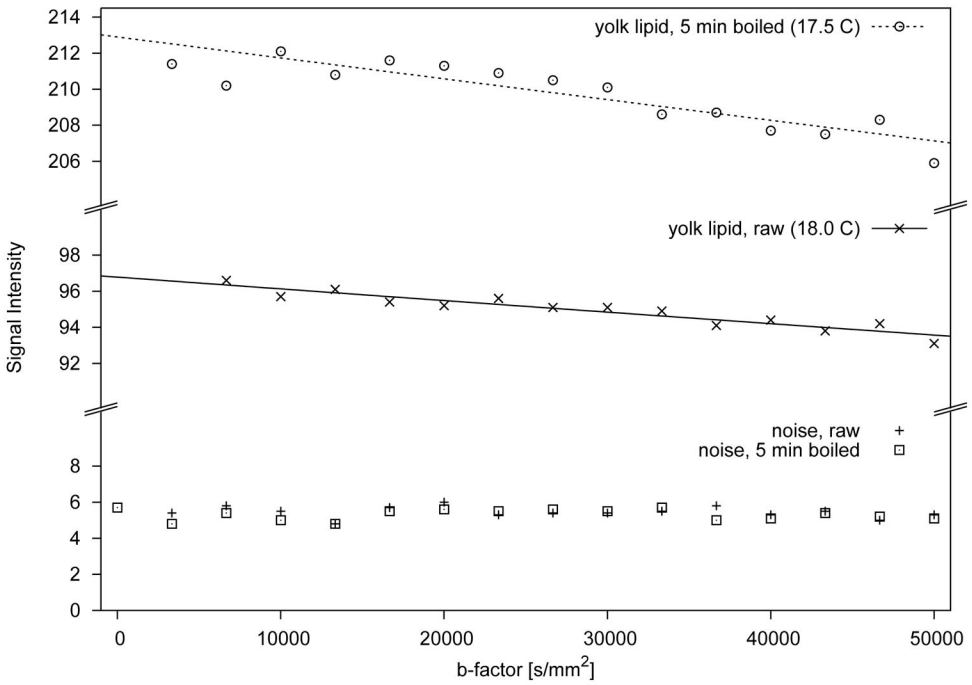

Figure 5.

Diffusion signal decay in yolk lipid ROIs measured with very high diffusion weighting ($5 \leq b \leq 50{,}000$ s/mm^2). The signal intensity scale has been split into three separate sections to better illustrate an exceedingly small diffusion dependent signal loss, despite very strong diffusion encoding. For a boiling time of 15 minutes, signal loss was even smaller and sometimes not evident at all and, therefore, reliable fits could not be obtained.

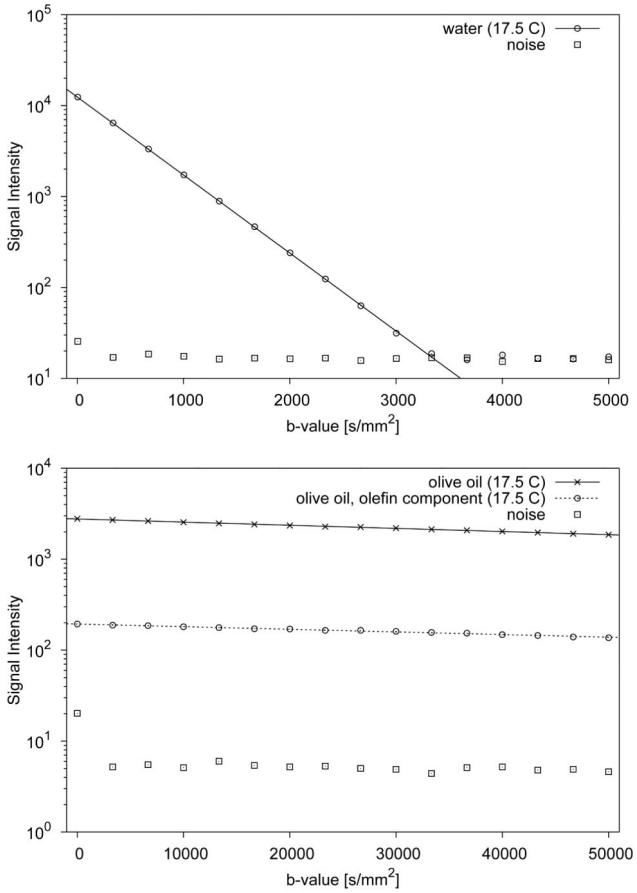

Figure 6.

Diffusion signal decay data of water (top graph) and olive oil (bottom graph). Water diffusion was measured with diffusion weighting between 5 to 5,000 s/mm^2. The slower diffusing olive oil was measured with diffusion weighting between 5 to 50,000 s/mm^2. For each *b*-value, average background noise is also shown. Continuous lines indicate monoexponential fits through the signal decay data.

Table 1

Average and standard deviation of fast and slow water diffusion coefficients and respective signal fractions measured in the latebra of raw and boiled chicken eggs. Values are presented for measurements without and with magnetization transfer (MT) pulse

Latebra (N=8, maximum b=5,000 s/mm^2, TE=85 ms)						
Boiling Time [min]	**MT**	**MT-Ratio [%]**	**D_1 [μm^2/ms]**	**D_2 [μm^2/ms]**	**f_1**	**f_2**
0	off		1.33±0.16	0.251±0.038	0.799±0.029	0.201±0.029
0	on	4.2± 1.5	1.35±0.18	0.263±0.045	0.789±0.029	0.211±0.029
5	off		1.42±0.19	0.286±0.042	0.793±0.046	0.207±0.046
5	on	5.2± 1.2	1.44±0.19	0.297±0.043	0.783±0.036	0.217±0.036
15	off		1.26±0.22	0.222±0.047	0.751±0.043	0.249±0.043
15	on	4.2± 4.2	1.28±0.21	0.232±0.042	0.740±0.039	0.260±0.039
p(MT on vs off, 0 min)			N.S.	<0.02	<0.05	<0.05
p(MT on vs off, 5 min)			N.S.	N.S.	N.S.	N.S.
p(MT on vs off, 15 min)			N.S.	N.S.	N.S.	N.S.
p(0 vs 5 min, MT off)			N.S.	N.S.	N.S.	N.S.
p(0 vs 15 min, MT off)			N.S.	N.S.	<0.05	<0.05
p(5 vs15 min, MT off)			N.S.	<0.01	N.S.	N.S.

Table 2

Average and standard deviation of diffusion coefficients and respective signal fractions measured in the latebra of raw and boiled chicken eggs. D_1, D_2, D_3, f_1, f_2, f_3 are diffusion parameters derived with triexponential analysis of diffusion data obtained with *b*-values between 5 and 50,000 s/mm^2, whereas D_1^M, f_1^M are diffusion parameters derived with monoexponential analysis of diffusion data obtained with *b*-values between 20,003 and 50,000 s/mm^2. Only measurements without magnetization transfer (MT) pulse are presented

Latebra (*N*=8, maximum *b*=50,000 s/mm^2, MT=off, TE=144 ms)								
Boiling Time [min]	D_1 [μm^2/ms]	D_2 [μm^2/ms]	D_3 [μm^2/ms]	f_1	f_2	f_3	D_3^M [μm^2/ms]	f_3^M
0	0.88±0.16	0.180±0.054	0.008±0.005	0.825±0.060	0.141±0.056	0.035±0.007	0.013±0.04	0.056±0.024
5	1.25±0.70	0.200±0.026	0.016±0.004	0.745±0.183	0.206±0.155	0.049±0.029	0.020±0.04	0.062±0.036
15[1]	-	-	-	-	-	-	0.006±0.03	0.112±0.036
p(0 vs 5 min)	N.S.	N.S.	<0.01	N.S.	N.S.	N.S.	<0.002	N.S.
p(0 vs 15 min)	-	-	-	-	-	-	<0.001	<0.005
p(5 vs 15 min)	-	-	-	-	-	-	<10^{-6}	<0.02

[1] Triexponential values are not reported, due to inconsistent convergence.

Magn Reson Med. Author manuscript; available in PMC 2014 August 01.

Table 3

Average and standard deviations of water ADCs measured in the egg white of raw and boiled chicken eggs. ADC values are presented for measurements without and with magnetization transfer (MT) pulse. The first ADC column represents values without temperature correction and the second ADC column values that have been extrapolated to a temperature of 20 Celsius

Egg White (N=8, maximum b=5,000 s/mm^2)				
Boiling Time [min]	**MT**	**MT-Ratio [%]**	**ADC [μm^2/ms]**	**ADC(20C) [μm^2/ms]**
0	off		1.76±0.07	1.77±0.02
0	on	5.8±0.7	1.76±0.07	1.77±0.02
5	off		1.62±0.12	1.65±0.04
5	on	21.8±2.8	1.63±0.15	1.67±0.04
15	off		1.62±0.07	1.65±0.02
15	on	22.7±3.6	1.62±0.07	1.66±0.03
p(0 vs 5 min, MT off)			<0.02	$<10^{-5}$
p(0 vs 15 min, MT off)			<0.002	$<10^{-6}$
p(5 vs 15 min, MT off)			N.S.	N.S.